14th International Conference on Applications of Statistics and Probability in Civil Engineering, ICASP14
Dublin, Ireland, July 9-13, 2023

Probabilistic safety-checking with un-scaled records for the equivalent SDOF system

Hossein Ebrahimian
Assistant Professor, Department of Structures for Engineering and Architecture, University of Naples Federico II, Naples, Italy

Fatemeh Jalayer
Professor, Institute for Risk and Disaster Reduction (IRDR), University College London, London, UK

Andrea Miano
Assistant Professor, Department of Structures for Engineering and Architecture, University of Naples Federico II, Naples, Italy

Fabrizio Mollaioli
Professor, Department of Structural and Geotechnical Engineering, University of Rome "La Sapienza", Rome, Italy

Andrea Prota
Professor, Department of Structures for Engineering and Architecture, University of Naples Federico II, Naples, Italy

ABSTRACT: The original N2 method employs the equivalent SDOF system of a MDOF structure to find the performance points associated to prescribed limit states. This procedure today forms the backbone of Eurocode and Italian code provisions for non-linear static analysis. To this end, a nonlinear dynamic analysis procedure dubbed as N2Cloud is explored. It is the application of Modified Cloud Analysis (a modified version of Cloud Analysis that has the capability of explicitly addressing the cases of global instability or numerical non-convergence) on an equivalent SDOF system. N2Cloud procedure is readily usable in the context of performance-based seismic assessment framework, where safety-checking can be performed at the level of the equivalent SDOF system. The 3D structural model of an existing five-story RC building located in L'Aquila (central Italy) is employed as a case-study. The structure in question has collapsed due to a soft-story mechanism in the L'Aquila 2009 earthquake. It is observed that safety-checking for the equivalent SDOF system leads to an extremely efficient yet vigorous and accurate estimates for this case-study compared to those obtained by MDOF system.

1. INTRODUCTION

The Italian Building Code (NTC 2018, Commentary, C7.3.4.2) provides a detailed procedure for non-linear static analysis (pushover curve is obtained by plotting base-shear versus roof displacement for a structure that is subjected to prescribed monotonically increasing static load patterns. The capacity curve is then mapped into an elastic-perfectly-plastic (EPP) equivalent single-degree-of-freedom (SDOF) system. The target displacement (a.k.a., the performance point) for the equivalent SDOF system is found by intersecting the inelastic design spectrum for a prescribed limit state and the equivalent EPP capacity curve. This procedure is in line with the N2 method proposed originally by Fajfar and Fischinger (1988) and its modified versions (e.g., Fajfar 2000; see also Fajfar 2021). However, the code provides the option for non-linear time-history analysis only for the multi-degree-of-freedom (MDOF) structure (NTC2018, §7.3.5). The present work investigates the use of the code-

based equivalent SDOF system in the non-linear dynamic response history analysis (NRHA). A nonlinear dynamic analysis procedure known as the Modified Cloud Analysis (MCA, Jalayer et al. 2017) is used for the equivalent SDOF system due to its simplicity and relatively small number of un-scaled records employed. MCA is a modified version of Cloud Analysis (CA) that has the capability of explicitly addressing the cases of global instability or numerical non-convergence under the so-called "collapse cases". The MCA procedure employed for the equivalent SDOF system is herein dubbed as *N2-Cloud* (Jalayer et al. 2019). This version of MCA is going to be particularly useful for analysis of systems with degrading backbone as it permits the analysis of the equivalent EPP system but properly handles, in the post-processing, the cases that go beyond a designated collapse threshold. By employing a system-level damage measure expressed in a critical demand to capacity ratio (*DCR*) format, N2-Cloud safety-checking is performed at the level of the equivalent SDOF system. DCR_{LS} (for a given limit state *LS*) permits the mapping of damage at the component level to the system level (Jalayer et al. 2009, 2017, and 2021; Miano et al. 2018); thus, a compatible definition is used for exceeding limit states at the component, system, and the equivalent SDOF levels. As a case-study, a 3D structural model of an existing five-story RC building with infills located in L'Aquila (central Italy) is used. This structure collapsed due to a soft-story mechanism in the L'Aquila 2009 earthquake. We have explicitly considered the interaction between flexure, shear and the axial forces and the rigid end rotation due to bar slip in the nonlinear modelling analysis of the building.

2. METHODOLOGY

2.1. Calculation of DCR_{LS} for the Equivalent SDOF

Four limit states are considered, namely, SLV-Infills (life-safety for infills), SLD (damage limitation), SLV (life safety) and SLC (near collapse). The latter three limit states are based on NTC2018. They are shown in Figure 1(c, d) for an example column and infill element. We separate the onset of different limit states in infills and RC frame members. SLV-Infills takes place when the first infilled panel in the whole building drops to 50% of the peak strength in the descending branch on its backbone curve. For RC frame members (columns and beams), and on the lateral component-based force-deformation response, SLC is defined as the point where a 20% drop in maximum resistance takes place. The onset of the SLV is defined with a deformation equal to 3/4th of that for the onset of SLC. The onset of SLD corresponds to the initiation of member yielding. The structural global collapse of the building can be reached if one of the following criteria takes place: (1) at least 50% of the columns in a story reach their ultimate deformational capacity (the component-level collapse, C, threshold is associated to the point having force equal to zero on the force-deformation backbone curve); (2) the drift of at least 50% of the columns in a story exceed 10%; (3) the maximum inter-story drift ratio measured at the center of mass of each story exceeds 10%. The onset of any given *LS* can be defined on the original pushover curve of the MDOF system, and then mapped into the equivalent EPP SDOF system. Figure 2 shows the onset of *LS*'s on the SDOF response in both global directions of the case-study building.

2.2. N2Cloud procedure

N2Cloud is the application of MCA procedure for the equivalent EPP SDOF instead of MDOF system. In the MCA procedure (Jalayer et al. 2017), the *N* data of DCR_{LS} values (*N*=number of ground motion waveforms) is partitioned into two parts: (a) "*NoC* data" or "cloud data" related to N_{NoC} non-collapse inducing records; (b) "*C* data" or "collapse data" correspond to N_C collapse-inducing records ($N_{NoC} + N_C = N$). The Fragility Assessment (FA) by MCA (i.e., estimating the analytical fragility curve) is based on Eq. (1), which is a weighted sum of two terms: (1) *CA-based fragility*: CA is applied to *NoC* data and the conditional lognormal distribution describes *LS* exceedance probability of the non-collapse-inducing records given the intensity measure *IM*

(see $\Phi(\cdot)$ in Eq. (1) as the standardized normal cumulative density function with the three parameters a, b, $\beta_{DCR|IM}$); (2) *unity*: the probability of exceeding a *LS* given that collapse has taken place. The weights (which sum to unity) are the probabilities $P(NoC|IM)$ and $P(C|IM) = 1-P(NoC|IM)$ that are defined by a bi-parametric logistic regression model (see Eq. 1, with the two parameters α_0 and α_1). Thus, the fragility has five model parameters $\boldsymbol{\chi}=[a, b, \beta_{DCR|IM}, \alpha_0, \alpha_1]$:

$$P\left(DCR_{LS}>1\middle|IM,\boldsymbol{\chi}\right)= \underbrace{\Phi\left(\frac{\ln\left(\overbrace{a\cdot IM^{b}}^{\eta_{DCR|IM}}\right)}{\beta_{DCR|IM}}\right)}_{\text{CA-based Fragility}}\times\underbrace{\left(\frac{e^{-\left(\alpha_0+\alpha_1\ln IM\right)}}{1+e^{-\left(\alpha_0+\alpha_1\ln IM\right)}}\right)}_{P(NoC|IM)}+1\times\underbrace{\left(\frac{1}{1+e^{-\left(\alpha_0+\alpha_1\ln IM\right)}}\right)}_{P(C|IM)=1-P(NoC|IM)} \quad (1)$$

The two terms $\eta_{DCR|IM} = a\cdot IM^b$ and $\beta_{DCR|IM}$ in Eq. (1) are conditional median and logarithmic standard deviation of DCR_{LS} for *NoC* data and for a prescribed *LS*. Figure 4 presents a complete picture of MCA procedure using the DCR_{LS} as the damage measure versus *IM*. The term $\eta_{DCR|IM}$ is described as a power-law function indicating linear relation in logarithmic scale (see grey-dotted line labeled as "CA regression" in Figure 4). Figure 4 shows the curve DCR^{50} (p=50%) with thick dark-blue line labeled as "MCA regression", and the curves DCR^{16} and DCR^{84} with dashed-blue lines (see Jalayer et al. 2017 for estimating the percentiles). To compare the parameters of the non-lognormal five-parameter MCA-based fragility curve (Eq. 1) with the lognormal fragility model, the equivalent lognormal parameters can be visually extracted from the MCA-based fragility curve. The median *IM* at the onset of *LS* (DCR_{LS}=1), $\eta_{IM|DCR=1}$, is the *IM* corresponding to 50% probability. The logarithmic standard deviation (dispersion) at the onset of *LS*, $\beta_{IM|DCR=1}$, is half of the logarithmic distance between *IM*'s corresponding to 16% and 84% probabilities (denoted as IM_C^{16} and IM_C^{84}) on the capacity (MCA-based fragility) curve. The two parameters $\eta_{IM|DCR=1}$ and $\beta_{IM|DCR=1}$ (reported in Figure 4 and shown in a visual format in Figure 5) can be interpreted as the parameters of an equivalent lognormal probability density function of *IM* at DCR_{LS}=1 (see thick-black line in Figure 4), whose cumulative distribution forms the fragility curve associated with the *LS* of interest.

2.3. Safety-checking

The Demand and Capacity Factor Design (DCFD, Cornell et al. 2002, Jalayer and Cornell 2003, Jalayer et al. 2020) is an analytical format derived for probabilistic performance-based seismic safety checking. It compares the seismic demand and capacity in probabilistic terms; the seismic demand is increased to account for the uncertainty in predicting the demand for an acceptable risk level, and the seismic capacity is decreased to consider the uncertainty in predicting the seismic capacity for a given *LS*. DCFD safety-checking format is based on rigorous probabilistic principles, which is generated from the risk-based statement of the performance objective for a prescribed *LS* that $\lambda_{LS} \le \lambda_a$, where λ_{LS} is the mean annual frequency of exceeding a given *LS* (a.k.a. seismic risk), and λ_a is an admissible risk level (associated with the considered *LS*). The *IM*-based DCFD is expressed by the closed- and analytical-form:

$$\underbrace{IM_{\lambda_a}\cdot e^{\frac{k}{2}\beta_{UH}^2}}_{F_D} \le \underbrace{\eta_{IM|DCR=1}\cdot e^{\frac{-k}{2}\left(\beta_{IM|DCR=1}^2+\beta_{UF}^2\right)}}_{F_C} \quad (2)$$

where F_D and F_C are the factored demand and factored capacity; IM_{λ_a} corresponds to the acceptable risk level λ_a through the median hazard curve λ_{IM} (the mean annual frequency of exceeding a given seismic intensity level); k is the slope of the linear approximation of λ_{IM} in the logarithmic scale; β_{UH} represents the (equivalent) *IM*-based epistemic uncertainty related to hazard assessment; β_{UF} is the logarithmic standard deviation representing the overall effect of epistemic uncertainties (i.e., modelling uncertainties and/or uncertainty in the fragility model parameters) on fragility assessment. Safety Ratio, $SR = F_D/F_C \le 1$, can be interpreted as a probabilistic quantification of the safety margin

between system-level demand and capacity (Jalayer et al. 2020). According to Eq. (2), the following issues are noted: (a) The *IM* at the onset of *LS* is expressed as a lognormal distribution with median $\eta_{IM|DCR=1}$ and logarithmic standard deviation $\beta_{IM|DCR=1}$ as defined in the previous section. (b) β_{UF} can be estimated as half of the (natural) logarithmic distance (along the *IM* axis) between the 84th and 16th percentile fragility curves, respectively (i.e., $\beta_{UF} = 0.5\ln(IM^{84}/IM^{16})$, where IM^{84} and IM^{16} are *IM*'s at the median (50% probability) from the fragility minus/plus one standard deviation, respectively (see Figure 5). To obtain the fragility curves with a certain confidence, one can refer to, e.g., Liel et al. (2009), Jalayer et al. (2015, 2017), or Jalayer and Ebrahimian (2020). Herein, for the numerical application in Section 2, we have used the concept of Roust Fragility (RF) proposed in Jalayer et al. (2017). (c) The median curve λ_{IM} is approximated by a power-law curve of the form $\lambda_{IM}(x) = k_o x^{-k}$ (see Figure 6). (d) β_{UH} can be estimated in the same manner as half of the logarithmic distance between hazard curves with 84% and 16% respectively and along the *IM* axis (see Figure 6). It is noted that both the slope k and β_{UH} are estimated at the onset of *LS* (DCR_{LS}=1), i.e., $\eta_{IM|DCR=1}$ (see Jalayer et al. 2020).

3. NUMERICAL APPLICATION

3.1. Case-study model description

The case-study structure, as shown in Figure 1(a, b), is a five-story RC moment-resisting residential building with masonry infills constructed in the 1960s in L'Aquila (central Italy), and was designed only for gravity loads. The structure was collapsed due to soft-story mechanism at 3rd floor in the L'Aquila 2009 earthquake. It lays on soil type B per the NTC 2018 with the average shear wave velocity of the upper 30m, V_{S30}=695m/s. The nonlinear modelling of the frame has been carried out using OpenSees version 3.3.0. The plasticity in structural elements is distributed over the plastic hinge length based on the force-based beam-column element (Beam with Hinges element) using the uniaxial Pinching4 material. The total lateral force-deformation response of the element considers the interaction between the shear, bar-slip, and the axial-flexural response. More details about this kind of nonlinear modelling of beam-column members can be found in Jalayer and Ebrahimian (2019) and Ebrahimian and Jalayer (2021).

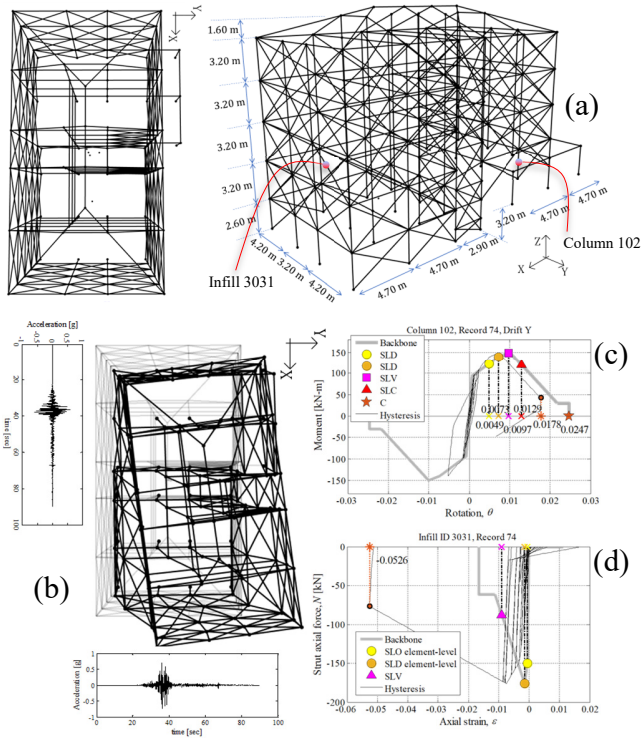

Figure 1: (a) Case-study building and the global axes; (b) final deformation of the case-study building subjected bidirectionally to M7.7 Chi-Chi 1999 Earthquake CHY028 (record 74 of the database); (c) the total monotonic moment-rotation response of column 102; (d) the axial force-strain of the equivalent truss element of the infill equivalent strut 3031 together with limit state thresholds and hysteretic responses for column and the infill equivalent strut.

For the infills, the model proposed by Liberatore et al. (2018) is used herein. According to this model, the shear versus horizontal displacement (or drift) backbone curve of infill is given by a multilinear curve defined by four characteristic points having different shear values, namely $0.40V_p$ (with V_p be the peak shear force), $0.85V_p$, V_p and zero. The effect of opening in

infills is considered based on correction factor proposed by Decanini et al. (2014), assuming that the infills contain unreinforced opening. We use Pinching4 material for nonlinear modelling of the infill, and the equivalent strut is modeled by a Truss Element. Figure 1(c, d) illustrates the component-level limit states based on NTC 2018 (C8.7.1.3) including SLD (orange circle), SLV (magenta square) and SLC (red triangle) for RC beam-columns (see Figure 1c) and also SLV-infills (magenta triangle, see Figure 1d), as discussed previously in Sections 1.1 and 1.2. The point marked as (C) with red start in Figure 1c shows the component-level collapse threshold (see Section 1.2). With reference to the hysteretic response in Figure 1c, building has global structural collapse due to numerical instability in NRHA of record 74.

3.2. Equivalent EPP SDOF system

The building in question has the 1st-mode period T_1=0.440sec (translation in Y-direction+rotation along Z-axis), and the 2nd-mode period T_2=0.351sec (translation in X-direction+rotation) considering that around 80% of the total building mass is participating in each of these two modes. To this end and following the provisions in the NTC 2018 (C7.3.4.3), we have used the load pattern proportional to the first and second mode-shapes to perform the pushover analyses in ±Y- and ±X- directions (we have not considered the mass-proportional load pattern, as this would not be a realistic situation for an irregular building). Then, the pushover curves (in terms of base shear versus roof displacement at the center of mass of the fifth story) on MDOF system are mapped into their equivalent SDOF systems (thick grey lines in Figure 2), and then they are converted to EPP models (solid black lines).

Figure 2 also shows the limit states on the equivalent EPP SDOF system, as discussed in Section 1.1 for both global X and Y directions. The hysteretic response due to record 74 are also shown on the figure indicating that the absolute maximum displacement exceeds the point C (red star) that corresponds to the structural global collapse. This message is in line with the results of global collapse of the MDOF system subjected to this record (see Figure 1). The equivalent period of the EPP systems are $T_1^* = 0.468$sec (Y-direction) and $T_2^* = 0.373$sec (X-direction), which are very close to T_1 and the T_2 of the MDOF system.

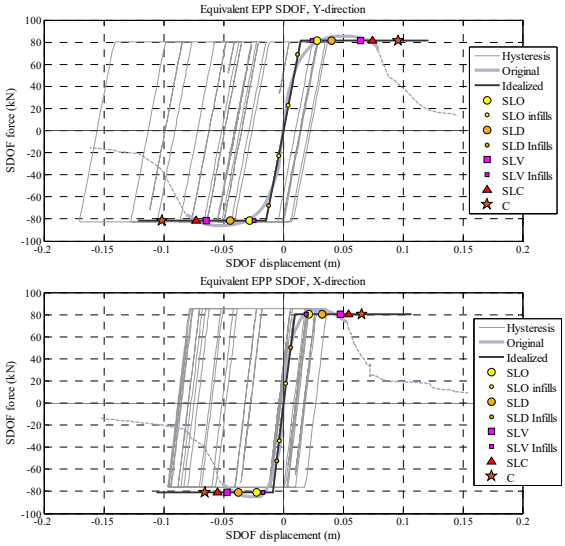

Figure 2: Equivalent SDOF system (labelled as original); the equivalent EPP system (labelled as idealized) and the limit states for two main directions (it is noted that the operational LS's SLO for frame, SLO- and SLD-infills are not considered in this study).

3.3. Fragility estimation: N2Cloud on EPP SDOF vs. MCA on MDOF systems

We have selected a large set of 81 ground-motion waveforms from different databases including: 57 records from NGA West2 (Ancheta et al. 2014); 11 from ITACA (Italian Accelerometric Archive, http://itaca.mi.ingv.it/) on the central Italy 2016 seismic sequence; 2 from International Institute of Earthquake Engineering and Seismology (IIEES, Dr. H. Zafarani, *personal communication*) on the Kermanshah M7.3 event; 11 from ESM (Engineering strong motion database, https://esm-db.eu/) including the February 2023 Turkey seismic sequence. These records have V_{S30}>360m/s (corresponding mainly to soil type B with a few on soil type A based on NTC 2018), $M_w \geq 4.7$, no limits on the source-to-site distance, and correspond to crustal focal mechanisms (reverse, strike-slip and normal faulting styles). Since the computational effort for the analysis of

an EPP-SDOF system is minimum, we took the liberty of choosing a large record set. Figure 3 shows that the set of records are quite spectrum compatible for SLV, so that the mean spectrum falls within the limit established by the NTC 2018 code (§3.2.3.6) as well as close to the uniform hazard spectrum (UHS) proposed by ESHM20 model (Danciu et al. 2021, see also http://hazard.efehr.org/). We have been particularly careful in maximizing the dispersion around the mean spectrum. Large dispersion in spectral acceleration values favors a more accurate estimation of the slope of regression.

Figure 4 shows the results of the two nonlinear dynamic analysis procedures, MCA (for MDOF system) and N2cloud (for equivalent EPP SDPF system), for the set of 81 ground motions and SLV limit state. The non-lognormal fragility model parameters $\boldsymbol{\chi}$=[a, b, $\beta_{DCR|IM}$, α_0, α_1] (see also Eq. 1) for both procedures are shown in the corresponding sub-figures and all the plot ingredients are fully descried in Section 1.3. For *IM*, we have considered the *Sa*RotD50 as 50th percentile (median) values of response spectra of the two horizontal components projected onto all nonredundant azimuths. This is in line with the definition of *IM* based on the ESHM20 hazard model. For the MCA, we have considered the geometric mean of *Sa*RotD50 at the first two periods T_1 and T_2 of the MDOS system. For N2Cloud, we have used T_1^* and T_2^* for the EPP SDOF system. Comparing the two sub-figures in Figure 4, the following key observations can be drawn: (1) The equivalent lognormal fragility parameters $\eta_{IM|DCR=1}$ and $\beta_{IM|DCR=1}$, reported in Figure 4, indicate that the median of the fragility curve can be properly estimated based on N2Cloud (=0.84) compared to MCA on MDOF system (=0.90g). Smaller dispersion in N2Cloud fragility manifests itself in the lower dispersion, $\beta_{DCR|IM}$, in the CA while using SDOF system compared to MDOF system. It should be noted that $N_C = 18$ for MCA and $N_C = 14$ for N2Cloud. The higher value of collapse cases in MCA procedure can also dictate the median to become smaller compared to N2Cloud procedure.

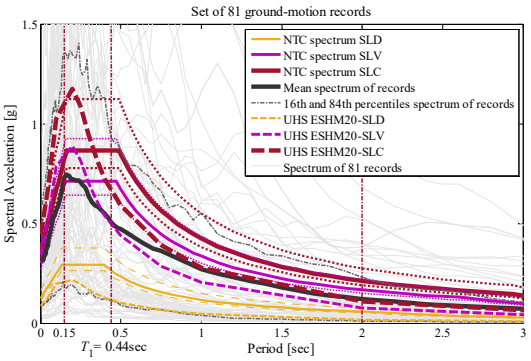

Figure 3: The mean spectrum and 16th and 84th percentile spectra for the suite of 81 records and comparison with the NTC2018 design spectra and ESHM20-UHS for SLD, SLV, and SLC limit states.

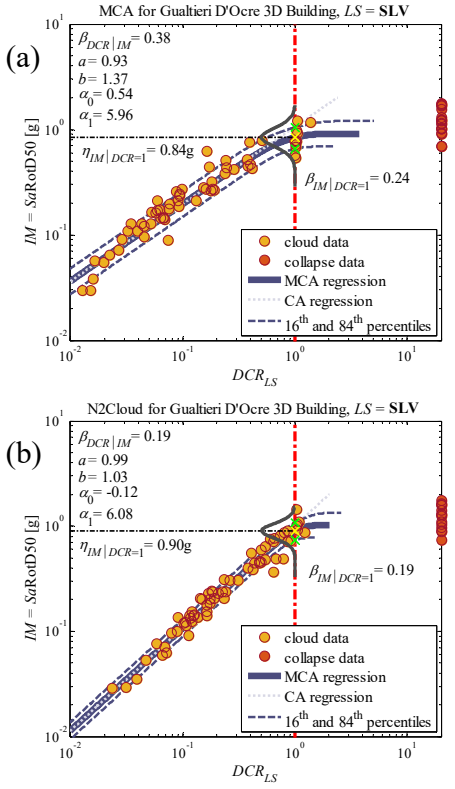

Figure 4: Graphical representation of (a) MCA and (b) N2Cloud procedures.

Figure 5 shows the RF curve for N2Cloud procedure (RF-N2Cloud; black solid line) with its standard deviation ($\pm 2\sigma$ confidence interval; shaded blue area), FA-N2Cloud (dashed magenta), and FA-MCA (solid magenta). The latter two are conventional approach of estimating the analytical fragility curve based on five-parameter model shown in Eq. (1). The RF

confidence band essentially indicates the error due to limited sample size (=81 herein). The fragility estimated based on MCA performed on the MDOF model falls within the 2 standard deviation confidence interval of the N2Cloud-based fragility estimated based on EPP-SDOF.

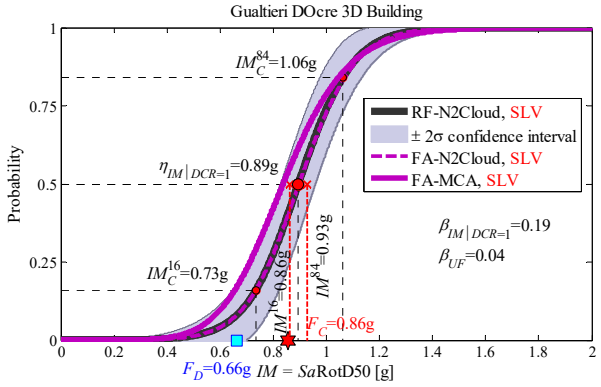

Figure 5: Comparing the fragility curves for SLV limit state associated with MCA and N2Cloud.

3.4. Safety-checking based on N2Cloud and MCA procedures.

All *IM*-based DCFD parameters, namely, IM_{λ_a}, k, $\eta_{IM|DCR=1}$, $\beta_{IM|DCR=1}$, β_{UF}, and β_{UH} (see Section 1.4), can be estimated visually from the fragility (Figure 5) and hazard (Figure 6) curves. Figure 6 shows the site-specific median hazard curve, λ_{IM}, and its 16th and 84th confidence interval, based on the ESHM20 hazard model for the building site. To avoid new hazard estimates, we consider the *IM* for the hazard curve to be *Sa*RotD50 at $T_1 = 0.44$sec or $T_1^* = 0.468$sec. The slope $k = 2.52$ is associated to the line fitted in the log scale at *IM* value corresponding to $\eta_{IM|DCR=1} = 0.89g$ based on Figure 5 (using N2Cloud procedure). $\beta_{UH} = 0.45$ is the epistemic uncertainty in the hazard curve visualized as the confidence band in Figure 6 measured in *IM* terms at $\eta_{IM|DCR=1}$. The acceptable rate $\lambda_a = -\ln(1 - P_{V_R})/50C_U$, where $C_U = 1.0$ for residential buildings and the exceedance probability in the reference time period $50C_U$ years is $P_{V_R} = [0.63, 0.10, 0.05]$ for SLD, SLV and SLC limit state (NTC 2018), and $P_{V_R} = 0.10$ for SLV-infills; thus, $\lambda_a = 0.0021$ for SLV, which corresponds to a return period of around 475 years. Thus, based on Eq. (2), $F_D = 0.66g$, and using the variables shown in Figure 5, $F_C = 0.86g$, and we will have $SR = F_D/F_C \cong 0.80$. Both F_D and F_C values are visualized in Figure 5, where it shows that the safety-checking criteria ($F_D \leq F_C$) is met for SLV limit state. The above results are derived based on N2Cloud procedure (using EPP-SDOF system). Table 1 compares the safety-checking results based on MCA procedure on the MDOF system as the accurate estimate with N2Cloud procedure and for all the four considered limit states. With reference to Table 1, it is revealed that F_D and F_C derived based on the two procedures (as a safety-checking measure) are quite similar and have the same trend. It is noted that employing N2Cloud diminishes the computational effort to a much lesser extent compared to the MCA on a MDOF system. The cases which do not meet the safety-checking criteria (i.e., $F_D > F_C$) are highlighted, showing that the criteria for SLV-Infills and also SLC limit states are not met.

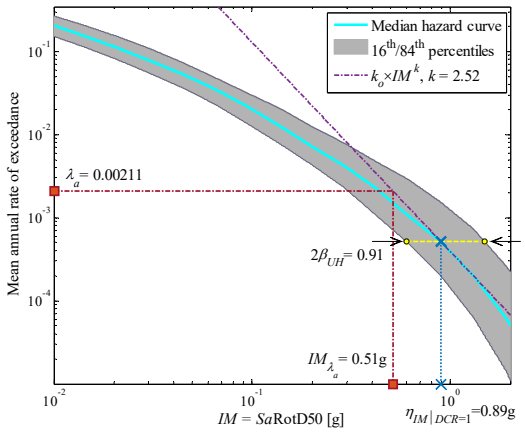

Figure 6: Site-specific median hazard curve with confidence interval.

Table 1: IM-based DCFD safety-checking results

		SLV-Infills	SLD	SLV	SLC
N2CLoud	$F_D(g)$	0.518	0.162	0.664	0.856
	$F_C(g)$	0.370	0.689	0.855	0.912
	SR	≅ 1.40	≅ 0.20	≅ 0.80	≅ 1.0
MCA	$F_D(g)$	0.560	0.171	0.550	0.885
	$F_C(g)$	0.408	0.658	0.795	0.826
	SR	≅ 1.40	≅ 0.30	≅ 0.70	≅ 1.10

4. CONCLUSIONS

"N2Cloud" is the modified Cloud Analysis (MCA) procedure for the equivalent EPP SDOF system. It can be used for fragility and risk assessment. Running on the SDOF system, it can efficiently reduce the running time of NRHA. The critical demand to capacity ratio (*DCR*), as a global damage measure, facilitates the identification of the limit state thresholds. It is shown that the N2Cloud safety-checking results are comparable and close to those provided by application of MCA on the complete MDOF system.

5. ACNOWLEDGEMENTS

The authors would like to acknowledge partial support from the PRIN-2017 MATISSE (Methodologies for the AssessmenT of anthropogenic environmental hazard: Induced Seismicity by Sub-surface geo-resources Exploitation) project no. 20177EPPN2 funded by the Italian Ministry of Education and Research.

6. REFERENCES

Ancheta, T.D., Darragh, R.B., Stewart, J.P., et al. (2014). NGA-West2 database. *Earthquake Spectra*, 30(3), 989-1005.

Cornell, C. A., Jalayer, F., Hamburger, R. O., and Foutch, D. A. (2002). Probabilistic basis for 2000 SAC federal emergency management agency steel moment frame guidelines. *Journal of structural engineering*, 128(4), 526–533.

Danciu, L., Nandan, S., Reyes, C., et al. (2021). *The 2020 update of the European Seismic Hazard Model: Model Overview*. EFEHR Technical Report 001, v1.0.0, DOI:10.12686/a15.

Ebrahimian, H., and Jalayer, F. (2021) Selection of seismic intensity measures for prescribed limit states using alternative nonlinear dynamic analysis methods. *Earthquake Engineering and Structural Dynamics*, 50(5), 1235-1250.

Fajfar, P., and Fischinger, M. (1988). N2-A method for non-linear seismic analysis of regular buildings. *In Proceedings of the ninth world conference in earthquake engineering*, Vol. 5, pp. 111-116.

Fajfar, P. (2000). A nonlinear analysis method for performance-based seismic design. *Earthquake spectra*, 16(3), 573-592.

Fajfar, P. (2021). *The Story of the N2 Method*. International association for earthquake engineering (IAEE).

Jalayer, F. and Cornell, C. A., 2003. *A technical framework for probability-based demand and capacity factor design (DCFD) seismic formats, Tech. Rep. PEER2003/08*, Pacific Earthquake Engineering Research Center (PEER), University of California Berkeley, CA.

Jalayer, F., De Risi, R., and Manfredi, G., 2015. Bayesian Cloud Analysis: efficient structural fragility assessment using linear regression, *Bulletin of Earthquake Engineering*, 13(4), 1183–1203.

Jalayer, F., Ebrahimian, H., Miano, A., Manfredi, G., and Sezen, H. (2017) Analytical fragility assessment using un-scaled ground motion records. *Earthquake Engineering and Structural Dynamics*, 46(15), 2639-2663.

Jalayer, F., Ebrahimian, H., and Miano, A. (2019). N2 with Cloud: A Non-Linear Dynamic Analysis Procedure for the Equivalent SDOF System. *XVIII Convegno ANIDIS L'ingegneria Sismica in Italia*, Ascoli Piceno, 15-19 settembre 2019, ID: 4548155. DOI: 10.1400/271224.

Jalayer, F, and Ebrahimian, H. (2019) Seismic reliability assessment and the nonergodicity in the modelling parameter uncertainties, *Earthquake Engineering and Structural Dynamics,* 49(5), 434-457.

Jalayer, F., Ebrahimian, H., and Miano, A. (2020) Intensity-based demand and capacity factor design: A visual format for safety checking. *Earthquake Spectra*, 36(4), 1952-1975.

Jalayer, F., Ebrahimian, H., and Miano, A. (2021). Record-to-record variability and code-compatible seismic safety-checking with limited number of records. *Bulletin of Earthquake Engineering*, 19(15), 6361-6396.

Liberatore, L., Noto, F., Mollaioli, F., and Franchin, P. (2018). In-plane response of masonry infill walls: Comprehensive experimentally-based equivalent strut model for deterministic and probabilistic analysis. *Engineering Structures*, 167, 533-548

Liel, A. B., Haselton, C. B., Deierlein, G. G., and Baker, J. W. (2009). Incorporating modeling uncertainties in the assessment of seismic collapse risk of buildings. *Structural Safety*, 31(2), 197–211.

Miano, A., Jalayer, F., Ebrahimian, H., and Prota, A. (2018). Cloud to IDA: efficient fragility assessment with limited scaling. *Earthquake Engineering and Structural Dynamics*, 47(5), 1124-1147.